Available online at www.sciencedirect.com

SCIENCE DIRECT®

Coastal Engineering 51 (2004) 697–711

Coastal Engineering
An International Journal for Coastal, Harbour and Offshore Engineers

www.elsevier.com/locate/coastaleng

A predictive relationship for the spacing of beach cusps in nature

Tsuguo Sunamura

Department of Earth and Space Sciences, Osaka University, Osaka, 560-0043, Japan

Available online 11 September 2004

Abstract

Modeling is carried out to obtain a relationship that enables the prediction of the spacing of beach cusps using wave and sediment parameters. The modeling is based on the concepts that: (1) the path of wave uprush flow diverging at a cusp horn has a close connection with the cusp spacing, and (2) the flow path is affected by the grain size of beach sediment. The following equation is derived: $\lambda = A\phi T\sqrt{gH}$, in which λ is the cusp spacing, H is the nearshore wave height, T is the wave period, ϕ is a dimensionless quantity representing the effect of sediment grain size: ϕ=exp($-0.23D^{0.55}$), where D is the grain size in mm-units, g is the gravitational acceleration, and A=1.35. The value of A is determined using a large amount of existing field data. Applicability of the predictive equation is examined by using the data from an embayed beach in New South Wales, Australia. The result indicates that this equation is capable of reasonably explaining a general trend of the alongshore variation in cusp spacings.

Keywords: Beach cusps; Cusp spacings; Prediction; Swash pattern; Sediment grain size

1. Introduction

One of the attractive morphologies along sandy or gravel shores are beach cusps, which are quasi-regularly spaced, rhythmic cuspidate features in the swash zone, frequently observed under calm sea conditions. Palmer (1834) first observed how the process of sediment movement leads to the development of beach cusps. Since then, various ideas, hypotheses and models on the origin, formation or development of this landform have been presented. Among these, a widely accepted model developed over two decades ago is the one proposed by Guza and Inman (1975): the edge wave model. Many field studies (e.g., Huntley and Bowen, 1978; Sallenger, 1979; Guza and Bowen, 1981; Inman and Guza, 1982; Seymour and Aubrey, 1985; Sherman et al., 1993; Allen et al., 1996) and laboratory experiments (Kaneko, 1985; Takeda et al., 1986) have supported this model, although most

E-mail address: sunamura@ess.sci.osaka-u.ac.jp.

0378-3839/$ - see front matter © 2004 Published by Elsevier B.V.
doi:10.1016/j.coastaleng.2004.07.004

of them have assumed "the presence of edge waves." Recent field studies (Holland and Holman, 1996; Masselink and Pattiaratchi, 1998; Masselink, 1999) and a laboratory study (Aoki and Sunamura, 2000) have provided no positive support for the model. Based on the self-organization theory, Werner and Fink (1993) presented a new model that was able to simulate the evolution of beach cusps. Coco et al. (1999a) who investigated the applicability of the self-organization model and the edge wave model by use of the previous field and laboratory data, have given no conclusive statement on the superiority of one model to the other. The compatibility of the two models has been examined through simulation studies by Coco et al. (1999b, 2000). The self-organization model has been tested in the field (Coco et al., 2003).

The edge wave model has provided the following predictive relationship for cusp spacings:

$$\lambda = (g/2m\pi)T^2\tan\beta \qquad \text{(I)}$$

where λ is the spacing of beach cusps, T is the wave period, β is the beach slope angle, g is the gravitational acceleration, m=1 for the case of zero-mode subharmonic edge waves, and m=2 for the zero-mode synchronous case (e.g., Guza and Inman, 1975; Inman and Guza, 1982). Eq. (I) predicts an increasing spacing with increasing slope for a constant wave period. Field measurements by Masselink (1999) along a 1-km-long embayed beach in New South Wales, Australia, with little local variation in wave period indicated no significant correlation between cusp spacing and beach slopes. The beach slope increases as grain size increases or as wave height decreases, when wave period is kept constant (Sunamura, 1984). Considering that the beach-slope factor in Eq. (I) includes implicitly the effects of wave height and sediment grain size on the cusp spacing, the equation suggests that the spacing should increase with increasing grain size or decreasing wave height. According to Dean and Maurmeyer (1980), however, this spacing vs. grain size relationship is contrary to field observations in northern California. Sunamura (1989) has also reported that the spacing vs. wave height relationship is opposite to field findings at various places. These facts make it difficult to accept Eq. (I) as an appropriate predictor for cusp spacing. A predictive formula should include explicitly factors of waves and sediment grain size.

The self-organization model by Werner and Fink (1993) yields the following relationship:

$$\lambda = fS \qquad \text{(II)}$$

where S is the swash excursion length and f is a coefficient, averaging 1.7. Dean and Maurmeyer (1980) have already derived the same relationship from a different model and obtained f=1.5 using data from northern California beaches. Through the analysis of field and laboratory data, Takeda and Sunamura (1983) have shown that an average value of f takes on 1.5; Coco et al. (1999a) have obtained f=1.63. A similar f-value, 1.57, was reported from a New South Wales beach in Australia (Masselink, 1999). The consistency in f-values strongly suggests positive support for the self-organization model, but it does not mean that Eq. (II) can serve as a predictive formula. This equation represents no causality, because both λ and S are dependent variables. Major controlling factors for λ are wave height, period, and sediment grain size; these also control the beach face slope (Sunamura, 1984), which in turn influences S.

Physical processes that determine the spacing of beach cusps are still unclear. It is known that the swash process is of crucial importance in controlling of cusp spacings. Considering that the spacing of equilibrated cusps is closely related to a swash flow deflected at a cusp horn, the present study attempts to develop a simple model, from which a predictive relationship for the cusp spacing will be derived.

2. Background

A recent field experiment by Sunamura and Aoki (2000), who used a suspended video-camera system to monitor continuously the process of cusp development from a manually flattened, plane section of a coarse clastic beach, indicated that cusps gradually and successively grew up along the beach section under the action of waves normal to the beach. A similar alongshore growth of beach cusps has been observed in a wave basin experiment (Aoki and

Sunamura, 2000) in which a planar model beach was exposed to normally incident waves. In the former field study, a topographic depression, probably caused by the presence of boulders at the end of the plane beach, triggered the cusp formation. In the latter laboratory study, locally increased intensity of swash action, probably induced by a local increase in wave height, resulted in landward bending of the crest of a berm with simultaneous occurrence of a minuscule depression on the model beach, which finally led to the formation of cusps. Werner and Fink's (1993) simulation study assumed such an incipient topographic low as a trigger for cusp development, which is comparable with descriptions in early studies by Johnson (1910), Kuenen (1948) and Russell and McIntire (1965). Various causes are considered for the incipience of a depression on the beach face. They are: the breaching of beach ridges or berms (Williams, 1973; Dubois, 1978; Sallenger, 1979; Pyökäri, 1982), the presence of boulders (Sunamura and Aoki, 2000), and local peaking of wave height, possibly induced by standing edge waves (Miller et al., 1989) or by intersecting waves (Dalrymple and Lanan, 1976; Aagaard, 1985).

An incipient depression acts to increase backwash flow, thereby accelerating erosion, which enlarges the depression to form an embayment, which later develops into a cusp bay. During the uprush phase, part of the water mass flowing up onto the sides of the embayment is deflected toward its central portion, so that the backwash flows decelerate to facilitate sediment deposition, eventually giving rise to the occurrence of cusp horns. This topographic high in turn would disturb the pattern of swash flow on a contiguous, still planar beach face, enhancing backwash flow, which leads to the formation of a new depression adjacent to the cusp horn, and the depression grows up to a cusp embayment in time. Thus, a topographic irregularity perturbs the structure of swash flow, resulting in morphological change. The interaction between morphology and flow structure, characterized by feedback relationships (Coco et al., 2003), propagates alongshore producing successively beach cusps with the spacings adjusted, although mechanisms for spacing adjustment are unclear at the moment.

The following characteristic flow pattern occurs in the cusp field: the uprush flow deflected by the cusp horn meets in the central portion of the embayment and recedes, enhancing the backwash flow, which results in retardation of the uprush of the next wave. This flow pattern, called 'horn-divergent flow' by Masselink and Pattiaratchi (1998), is similar to the one already reported from the cusp field at various places (e.g., Bagnold, 1940; Sallenger, 1979; Pyökäri, 1982; Dean and Maurmeyer, 1980; Holland and Holman, 1996; Masselink et al., 1997; Sunamura and Aoki, 2000), and is probably instrumental in maintaining cusp configurations (Masselink and Pattiaratchi, 1998). It is evident that horn-deflected swash pattern plays a crucial role in determining the spacing of beach cusps. With this flow pattern in mind, modeling will be conducted.

3. Modeling

Most of the beach cusps in the field are formed by normally approaching waves. They grow with the gradual emergence of a horn-divergent swash pattern (Sunamura and Aoki, 2000; Coco et al., 2003) and finally attain equilibrium. Modeling will be done considering fully developed cusps on a plane beach with such a flow pattern. The idea is similar to those of Dean and Maurmeyer (1980) and Masselink and Pattiaratchi (1998), but a different approach will be taken.

Let us first consider a deflected flow trajectory, represented by the angle θ, on an ideal beach having an impermeable, smooth, uniform slope with an angle of β (Fig. 1). Particle mechanics leads to the

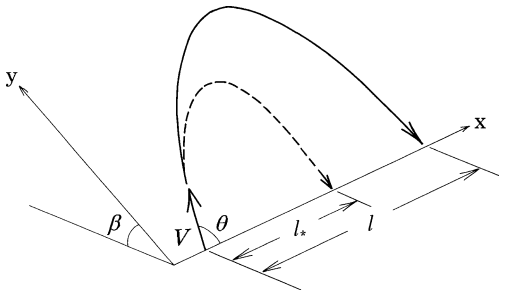

Fig. 1. Definition sketch. The solid curve denotes the trajectory of a water particle moving up obliquely on an impermeable, smooth slope. The dashed curve indicates an assumed parabolic path on a permeable, rough slope.

following equation for the maximum displacement of the water particle in the alongshore direction (the x-direction in Fig. 1), l, if the effect of friction is neglected:

$$l = V^2 \sin 2\theta / g \sin\beta \tag{1}$$

where V is the initial velocity of the water particle, and g is the gravitational acceleration.

Waves running up on the ideal beach without deflection (θ=90°) will be considered next. Again, neglecting the frictional effect, the maximum runup height, R, of a water particle with an initial velocity of V can be described as

$$R = V^2/2g \tag{2}$$

which is derived from a simple relation: ρgR (potential energy)=$\rho V^2/2$ (kinematic energy), where ρ is the density of water. According to Hunt (1959), the maximum height of waves running up on a beach of a porous, rough, uniform slope with an angle of β is given by

$$R = 2.3\phi T\sqrt{H}\tan\beta \ (\text{ft} - \text{sec}) \tag{3}$$

where T is the wave period, H is the nearshore wave height, and ϕ is a dimensionless coefficient expressing the ratio of runup height on a rough, permeable slope to that of a smooth, impermeable slope with the same gradient, i.e., a measure for the effectiveness of beach material in dissipating energy of runup waves. This relation holds when a ft-sec unit is applied. The following equation is dimensionally corrected using g:

$$R = k\phi T\sqrt{gH}\tan\beta \tag{4}$$

where k=0.41. Hunt (1959) has shown that ϕ is a function of the grain size of beach material, but unfortunately he has provided no functional relationship. The plot in Fig. 2 uses the data of Savage (1959), in which the x-axis denotes the sediment grain size, D, with a unit of mm and the y-axis indicates ϕ. The value of ϕ decreases with increasing grain size irrespective of the beach slope; the general trend is well expressed by the following

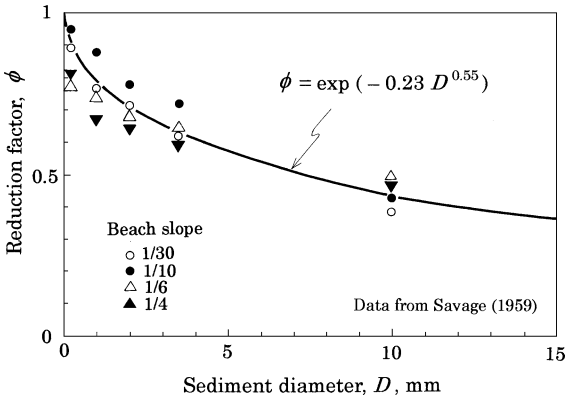

Fig. 2. A measure for the effectiveness of sediments working as a wave-energy dissipater, ϕ, plotted against the sediment grain size in millimeters, D.

exponential function, although some scatter of data points is found:

$$\phi = \exp\left(-0.23D^{0.55}\right) \tag{5}$$

It should be noted that ϕ is a dimensionless quantity but D has a mm-unit.

Let us examine the deflected flow trajectory (with the angle θ) on a permeable, rough, uniformly inclined beach (with the angle β). Assuming that the water particle motion follows a parabolic path as shown by the dashed curve in Fig. 1, the maximum lateral displacement of the water particle, l_*, can be obtained from Eqs. (1) (2) and (4) as

$$l_* = 2k\phi T\sqrt{gH}\tan\beta\sin 2\theta/\sin\beta \tag{6}$$

Since the shore with fully developed cusps has generally a small beach face angle, $\tan\beta \approx \sin\beta$. Transformation of Eq. (6) using this approximation yields

$$l_* = B\phi T\sqrt{gH} \tag{7}$$

where B=2 $k\sin 2\theta$. Similar to Dean and Maurmeyer (1980), the present study also assumes that the spacing of beach cusps is linearly related to l_* (Fig. 3).

$$\lambda = al_* \tag{8}$$

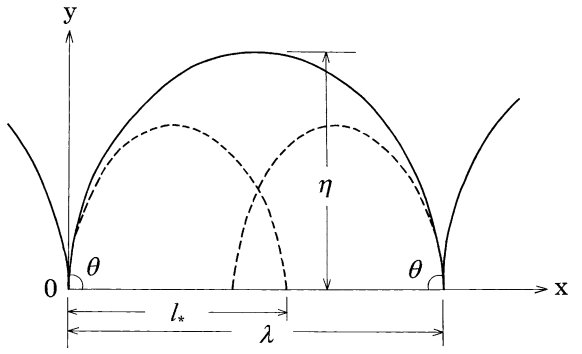

Fig. 3. Definition sketch. The solid and dashed curves denote a plan shape of beach cusps and a water-particle trajectory, respectively.

where a is a proportional coefficient. From Eqs. (7) and (8), we obtain

$$\lambda = A\phi T\sqrt{gH} \tag{9}$$

where

$$A = aB = 2ak\ \sin 2\theta = \text{constant} \tag{10}$$

if we consider a and θ being constants. Given wave characteristics (H, T) and the sediment parameter (ϕ in Eq. (5)), prediction of the cusp spacing is possible once A is known.

Assuming that a plan shape of beach cusps can be expressed by a parabola as shown by the solid curve in Fig. 3

$$y = \tan\theta(1 - x/\lambda)x \tag{11}$$

and inserting $x=\lambda/2$ and $y=\eta$, we have

$$\eta/\lambda = (\tan\theta)/4 \tag{12}$$

where η is the maximum cusp indentation (Fig. 3), which Nolan et al. (1999) called a "beach cusp depth." The quantity η/λ is a parameter for representing the prominence of a cusp plan shape.

4. Determination of A-value

The cusp formation is most favorable under reflective beach conditions in which waves usually break in the mode of surging or collapsing, sometimes plunging. The height of these breakers can be reckoned as the nearshore wave height H, so that an approximation of $H \approx H_b$ (=the breaker height) will be applied in the following data-treatment. Sediment grain size with units of mm can be converted to the dimensionless ϕ-value using Eq. (5).

Prior to determination of the value of A in Eq. (9), effectiveness of the functional form of Eq. (9) will be examined using the data of laboratory experiments (Table 1) conducted under simplified conditions: employment of regular waves, a constant water level, and sediments with unimodal distribution. The cusp spacing λ is plotted against the wave-sediment parameter $\phi T\sqrt{gH}$ in Fig. 4, which shows that the cusp spacing increases as the value of the wave-sediment parameter increases: the functional form is found to be valid. Fig. 4 illustrates that the value of A ranges from 0.4 to 0.9, averaging A=0.65 for the laboratory.

Then, field data (Table 2) were used to obtain the value of A to be applied to the full-scale environment; significant wave parameters were employed to plot the data in Fig. 5. The A-value falls in a range from 0.7 to 2 if we neglect three outlying data points (arrowed); the average value is 1.35. Using Eq. (9) with this value enables the prediction of the spacing of beach cusps in the field.

The value of A for the field, 1.35, is almost twice as large as that for the laboratory, 0.65. This difference could probably be ascribed to the fact that beach cusps in the field are formed by irregular waves with variable heights and periods, while laboratory cusps are formed by regular waves with a constant height and period. According to field observations, higher and longer waves in a train of waves acting on a beach to form cusps are likely to contribute more to their formation and maintenance. This suggests that waves with larger heights and longer periods, compared to significant waves, actually control the spacing of beach cusps. With reference to the plot of Fig. 5, using such wave data must have caused a rightward shift of the overall data points, resulting in a reduction of the A-value. Quantitative discussion on this point is left for a future study.

Table 1
Summary of previous laboratory data

Author(s)	λ (cm)	D (mm)	ϕ	H (cm)	T (s)	$\phi T\sqrt{gH}$(cm)	Remarks
Ann (1979)	20	0.2	0.91	0.91[a]	0.85	41.9	
	17	0.2	0.91	2.8[a]	0.78	37.2	
	24	0.2	0.91	4.1[a]	0.86	49.6	
	24	0.2	0.91	4.1[a]	0.79	45.6	
Aoki and Sunamura (2000)	11.1	1.3	0.76	0.55[b]*	0.84	14.8	*Measured at
	11.2	1.3	0.76	0.60[b]*	0.84	15.5	15-cm water depth
	12.0	1.3	0.76	0.80[b]*	0.84	17.9	
	12.1	1.3	0.76	0.90[b]*	0.84	18.9	
	12.5	1.3	0.76	1.00[b]*	0.84	20.0	
	14.0	1.3	0.76	0.95[b]*	1.00	23.2	
	14.0	1.3	0.76	1.00[b]*	1.00	23.8	
	14.5	1.3	0.76	1.10[b]*	1.00	24.9	
	15.8	1.3	0.76	1.40[b]*	1.00	28.1	
	16.5	1.3	0.76	1.65[b]*	1.00	30.6	
	20.6	1.3	0.76	1.80[b]*	1.00	32.0	
	20.2	1.3	0.76	1.95[b]*	1.00	33.2	
	20.0	1.3	0.76	2.00[b]*	1.00	33.7	
	21.5	1.3	0.76	1.30[b]*	1.22	33.1	
	22.2	1.3	0.76	1.40[b]*	1.22	34.4	
	22.3	1.3	0.76	1.50[b]*	1.22	35.6	
	22.8	1.3	0.76	1.70[b]*	1.22	37.8	
	23.6	1.3	0.76	1.80[b]*	1.22	38.9	
	25.5	1.3	0.76	1.90[b]*	1.22	40.0	
	24.8	1.3	0.76	2.20[b]*	1.22	43.0	
	24.5	1.3	0.76	2.30[b]*	1.22	44.0	
Aoki and Sunamura (Unpub.)	31.3	1.3	0.76	1.6[b]*	1.5	45.1	*Measured at
	28.5	1.3	0.76	1.9[b]*	1.5	49.2	15-cm water depth
	32.0	1.3	0.76	2.2[b]*	1.5	52.9	
	32.5	1.3	0.76	2.2[b]*	1.5	52.9	
	32.4	1.3	0.76	2.5[b]*	1.5	56.4	
	31.0	1.3	0.76	2.6[b]*	1.5	57.5	
	29.9	1.3	0.76	2.7[b]*	1.5	58.6	
	32.6	1.3	0.76	2.9[b]*	1.5	60.8	
	32.3	1.3	0.76	3.2[b]*	1.5	63.8	
	33.0	1.3	0.76	3.5[b]*	1.5	66.8	
	33.3	1.3	0.76	3.8[b]*	1.5	69.6	
	35.0	1.3	0.76	4.1[b]*	1.5	72.3	
	34.0	1.3	0.76	4.2[b]*	1.5	73.1	
	34.8	1.3	0.76	4.6[b]*	1.5	76.5	
Sunamur Ann (1979)	13.0	0.2	0.91	1.3[a]	0.56	18.2	
	11.6	0.2	0.91	1.5[a]	0.56	19.5	
	15.7	0.2	0.91	2.0[a]	0.56	22.6	
	15.3	0.2	0.91	2.2[a]	0.56	23.7	
	15.6	0.2	0.91	2.8[a]	0.56	26.7	
Takeda and Sunamura (1983)	34.0	0.69	0.83	4.2[a]	1.0	53.2	
	20.0	0.69	0.83	2.0[a]	1.0	36.7	
Takeda et al. (1986)	10.0	0.69	0.83	0.6[a]	0.8	16.1	
	13.0	0.69	0.83	0.7[a]	0.9	19.6	
	12.5	0.69	0.83	10.0[a]	0.9	23.4	
	12.9	0.69	0.83	1.0[a]	0.9	23.4	
	13.0	0.69	0.83	1.1[a]	0.9	24.5	
	16.0	0.69	0.83	1.3[a]	1.0	29.6	
	17.0	0.69	0.83	1.4[a]	1.0	30.7	

Table 1 (*continued*)

Author(s)	λ (cm)	D (mm)	ϕ	H (cm)	T (s)	$\phi T\sqrt{gH}$(cm)	Remarks
Takeda et al. (1986)	23.0	0.69	0.83	0.8[a]	1.2	27.9	
	20.0	0.69	0.83	0.9[a]	1.2	29.6	
	23.0	0.69	0.83	1.8[a]	1.2	41.8	
	10.0	1.3	0.76	1.3[a]	0.8	21.7	
	12.5	1.3	0.76	1.8[a]	0.9	28.7	
	12.5	1.3	0.76	1.0[a]	0.9	23.8	
	12.5	1.3	0.76	13[a]	0.9	24.4	
	20.0	1.3	0.76	1.4[a]	1.2	33.8	
	20.0	1.3	0.76	1.5[a]	1.2	35.0	
	20.0	1.3	0.76	1.8[a]	1.2	38.3	
	20.0	1.3	0.76	2.1[a]	1.2	41.4	
Tamai (1980)	221	0.28	0.89	7.5[a]	2.20	168	
	173	0.28	0.89	12.6[a]	2.19	217	
	128	0.28	0.89	11.3[a]	1.78	168	
	140	0.28	0.89	12.8[a]	1.80	179	
Terasaki, Takeda and Sunamura (Unpub.)	40	0.69	0.83	4.0[a]	0.95	49.4	
	33	0.69	0.83	4.5[a]	0.95	52.4	
	42	0.69	0.83	4.3[a]	1.05	56.6	
	49	0.69	0.83	3.6[a]	1.25	61.6	
	51	0.69	0.83	4.5[a]	1.25	68.9	
	51	0.69	0.83	5.0[a]	1.25	72.6	
	71	0.69	0.83	6.0[a]	1.25	79.6	
	60	0.69	0.83	6.3[a]	1.25	82.2	
	56	0.69	0.83	6.5[a]	1.25	82.8	
	63	0.69	0.83	4.2[a]	1.48	78.8	
	66	0.69	0.83	3.5[a]	1.71	83.1	
	72	0.69	0.83	2.8[a]	1.94	84.3	
	85	0.69	0.83	4.3[a]	1.94	1.5	
	31	0.69	0.83	1.3[a]	2.30	68.0	
	40	069	0.83	2.0[a]	2.30	84.5	
	48	0.69	0.83	2.6[a]	2.30	96.4	
	50	0.69	0.83	4.1[a]	2.30	121	
	68	0.69	0.83	4.6[a]	2.30	128	
	75	0.69	0.83	2.2[a]	2.51	96.7	
	70	0.69	0.83	2.7[a]	2.51	107	

Laboratory experiments by Longuet-Higgins and Parkin (1962), Guza and Inman (1975), Dalrymple and Lanan (1978), and Guza and Bowen (1981) did not provide data of grain size of sand that they used, so their data are excluded.

[a] Breaking waves.

[b] Shallow-water waves.

Comparison between the laboratory (Fig. 4) and field results (Fig. 5) indicates that the field data are more scattered. The larger scatter can be attributed to the influences of: (1) tidal fluctuations, (2) temporally changing wave climate, (3) spatial and temporal variability of beach sediment size, and (4) variation in the spacing of beach cusps in nature.

According to an extensive data set collected by Nolan et al. (1999) from various beaches around the South Island in New Zealand, an average value of η/λ is 0.46 (Nolan et al., 1999). Laboratory data of Aoki and Sunamura (2000) show that η/λ averages 0.15 although the number of data is rather limited. This strongly suggests that beach cusps in the field have more prominence in shape than those in the laboratory. Larger cusp protrusion in the field would be due to the influences of tidal fluctuations, irregular waves, variable grain size of sediment, etc. Substituting the field value, η/λ=0.46, into Eq. (12), one obtains θ=62°. Using this value together with A=1.35 and k=0.41, Eq. (10) gives a=2. The result is

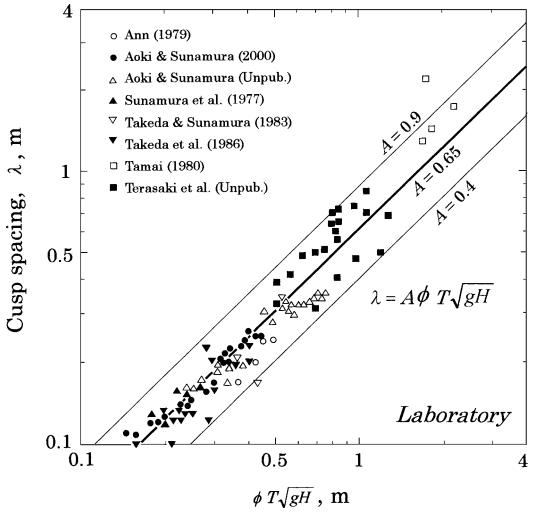

Fig. 4. Laboratory relationship between the cusp spacing, λ, and the wave-sediment parameter, $\phi T\sqrt{gH}$.

consistent with the value that Dean and Maurmeyer (1980) adopted in their cusp study on the California coast.

5. Application and discussion

Applicability of the predictive relationship (Eq. (9)) will be tested using field data collected by Masselink (1999) from Pearl Beach in Broken Bay, New South Wales, Australia (Fig. 6a). He discussed alongshore variations in beach cusp morphologies including the cusp spacing, in connection with swash excursion distance, beach face gradient, etc. According to Masselink (1999), the beach is characterized by: (1) a 1-km-long, south–north-oriented, zeta-shaped shoreline, (2) offshore wave climate of a dominant southeasterly swell superimposed on local wind waves, (3) the energy level of waves at the shoreline decreasing from the exposed northern section to the sheltered southern area by a headland named Green Point, (4) beach sediment size changing from coarse sand in the northern area to fine sand at the southern end, and (5) semidiurnal tides with a mean tidal range of 1.2 m. Post-storm, moderate, and constant waves with an offshore significant height of 1.5 m and a period of 8–9 s acted on the beach during the cusp formation and also during the measurement of cusp features by Masselink (1999).

Application of Eq. (9) requires knowledge of the alongshore distribution of wave height at the time of the cusp formation. To estimate the height distribution, deepwater waves with a height of 1.5 m and a period of 8.5 s, incident from southeast, were selected as representative of waves responsible for the event. A hydrographic chart "Broken Bay" (Australian Hydrographic Office, 1977) was prepared; underwater contours were drawn on the chart by smoothing out their small irregularities. No tidal fluctuations were considered here, water level being fixed at MSL, 0.9 m above the chart datum. This study further assumes for simplicity that: (1) waves arriving at the exposed northern section of the beach undergo refraction and shoaling, and those reaching the protected southern area experience diffraction, and (2) there is no area affected by the combined effect of refraction and diffraction.

For construction of a refraction diagram, the orthogonal method (e.g., Coastal Engineering Research Center, 1984) was employed. Orthogonals for offshore waves incident from SE with an 8.5 s period were plotted in Fig. 6b and c, the latter showing a detail refraction pattern in a shallower region landward of a 15-m contour. Fig. 6c also indicates an x-axis on the shoreline, originating from the southern end of Pearl Beach. Alongshore wave heights estimated at a water depth of 2 m were used for H in Eq. (9). This water depth is equal to the breaking depth estimated (e.g., Coastal Engineering Research Center, 1984) for the representative incident waves to the beach with a nearshore gradient of 1/10 (see Masselink, 1999, Fig. 2). Wave height estimation along the shoreline north of x=320 m was made taking account of both wave refraction and shoaling; the refraction coefficient, K_r, was obtained from Fig. 6c and the shoaling coefficient, K_s, was estimated at a water depth of 2 m based on linear wave theory. Nearshore wave height H was calculated through $H=K_rK_sH_o$, where H_o is the offshore wave height (=1.5 m). The result is listed in Table 3.

Wave heights near the shore south of x=320 m were estimated considering the effect of wave diffraction alone. Considering Green Point as a semi-infinite impermeable breakwater with waves approaching normal to it, the diffraction coefficient, K_d, at a location with 2 m water depth was obtained from a wave diffraction diagram (e.g., Wiegel, 1964,

Table 2
Summary of previous field data

Author(s)	λ (m)	D (mm)	ϕ	H (m)	T (s)	$\phi T\sqrt{gH}$(m)	Remarks
Allen et al. (1996)	27.5	0.47	0.86	0.48[a,*]	16.7	31.1	Canaveral National Seashore, Florida, USA *Measured at 1.5-m water depth
Dean and Maurmeyer (1980)	23.2	0.2	0.91	0.34[b]	15.4	25.5	Drakes Beach, California, USA
Dubois (1978)	35.0	0.31	0.89	0.6[b]	10	21.6	South of Café Henlopen, Delaware, USA
Dubois (1981)	32.5	0.33	0.88	1.3[b,*]	9**	28.3	Rehoboth Beach, Delaware, USA *Largest value during study period **Average value of 7–11 s
Holland and Holman (1996)	36*	0.36	0.87	3.5[a,**]	10.9	55.5	Duck, North Carolina, USA *1-m contour configuration **Measured at 8-m water depth
	29*	0.36	0.87	2.5[a,**]	11.2	48.2	
	32*	0.36	0.87	1.8[a,**]	10.6	38.7	
	36*	0.36	0.87	1.7[a,**]	11.5	40.8	
	40*	0.36	0.87	1.7[a,**]	14.2	50.5	
	37*	0.36	0.87	1.2[a,**]	13.5	40.3	
	20*	0.36	0.87	0.8[a,**]	11.3	27.5	
Krumbein (1947)	66.6	0.83	0.81	1.84[b]	9.3	31.8	HalfmoonBay, California, USA
	54.6	0.60	0.84	1.85[b]	9.8	35.0	
	52.5	0.51	0.85	1.81[b]	8.8	34.1	
	52.2	0.34	0.88	1.58[b]	9.9	34.3	
	52.5	0.23	0.90	1.37[b]	8.7	28.7	
	44.7	0.90	0.80	1.88[b]	12.5	42.9	
	44.1	0.51	0.85	1.88[b]	10.7	39.0	
	45.9	0.27	0.89	1.40[b]	11.1	36.6	
Longuet-Higgins and Parkin (1962)	4.3	14.0*	0.37	0.46[b]	6.2	4.9	Chesil Bank, England, UK *Average value of 2.54–25.4 mm
	5.5	14.0*	0.37	0.7[b]	6.1	6.1	
	4.3	14.0*	0.37	0.30[b]	5.4	3.4	
	3.7	14.0*	0.37	0.23[b]	6.2	3.4	
	4.0	14.0*	0.37	0.08[b]	6.9	2.2	
	10.1	14.0*	0.37	1.07[b]	5.0	6.0	
	6.4	14.0*	0.37	0.46[b]	6.3	5.0	
	6.4	14.0	0.37	0.38[b]	6.3	4.5	
	8.8	14.0	0.37	0.76[b]	6.2	6.3	
Masselink (1999)	28	0.45	0.86	1.25[b]	8.5*	25.6	North end at Pearl Beach, NSW, Australia *Average value of 8-9 s
	12	0.28	0.89	0.25[b]	8.5*	11.8	South end at Pearl Beach, NSW, Australia
Masselink and Pattiaratchi (1998)	30	0.4	0.87	0.3[a,*]	10	14.9	City Beach, Western Australia, Australia *Measured at 0.5-m water depth
	40	0.5	0.85	0.45[a,*]	13	23.2	Myalup Beach, Western Australia, Australia
	20	0.5	0.85	0.4[a,*]	11	18.5	*Measured at 0.5-m water depth
Masselink et al. (1997)	30	0.4*	0.87	0.7[b,**]	8	18.2	City Beach, Western Australia, Australia *Average value of 0.3–05 mm **Obtained with Komar and Gaughan's (1972) relation using deep-water wave height calculated from surf similarity parameter ξ=1.5
Sato et al. (1981)	15.2	0.7	0.82	1.0[b]	6.5	16.6	Motte, Kagoshima, Japan
Seymour and Aubrey (1985)	40	0.23	0.90	0.6[a,*]	16	35.0	Santa Barbara, California, USA *Measured at 9-m water depth
Sherman et al. (1993)	22.5*	0.2**	0.91	0.6[b,***]	6.5	14.3	Portmore Beach, Malin Head, Ireland *Average value of 20–25 m **Average value of 0.15–0.25 mm ***Obtained with Komar and Gughan's (1972) Relation using deep-water wave Height calculated from surf similarity parameter ξ=1.5

(continued on next page)

Table 2 (*continued*)

Author(s)	λ (m)	D (mm)	ϕ	H (m)	T (s)	$\phi T\sqrt{gH}$(m)	Remarks
Sunamura and Aoki (2000)	2.35	40	0.17	0.5[b]	6	2.2	Manazuru, Kanagowa, Japan
Takeda and Sunamura (1983)	21	0.28	0.89	0.98[b]	9.2	25.4	Naka Beach, Ibaraki, Japan
	15	0.28	0.89	0.76[b]	8.4	20.4	
	25	0.28	0.89	0.86[b]	7.8	20.1	
	22	0.28	0.89	1.48[b]	9.8	33.2	
	17	0.28	0.89	0.74[b]	6.5	15.6	
	15	0.28	0.89	0.66[b]	6.3	14.2	
	19	0.28	0.89	0.48[b]	5.6	10.8	
	28	0.30	0.89	1.54[b]	9.2	31.8	
	22	0.30	0.89	0.99[b]	6.5	18.0	
	16	0.30	0.89	0.90[b]	6.3	16.6	
	35	0.33	0.88	1.65[b]	8.0	28.3	
	20	0.33	0.88	0.90[b]	6.3	16.5	
Takeda and Sunamura (Unpub.)	11.0	0.29	0.89	0.34[b]	3.4	5.5	Kenbutsu, Takeyama, Japan
	15.9	0.19	0.91	0.30[b]	8.0	12.5	Okino-su, Tokushima, Japan
	14.3	0.21	0.91	0.30[b]	8.0	12.5	
Tamai (1980)	33.6	5.05	0.56	2.34[b]	9	24.1	Hisaeda, Kochi, Japan
	17.2	5.05	0.56	0.96[b]	10	17.2	
	16.5	5.05	0.56	0.76[b]	9.9	15.1	
	18.5	5.05	0.56	0.91[b]	9.9	16.6	
	16.5	5.05	0.56	0.75[b]	9.2	13.9	
	15.0	11.3	0.41	0.76[b]	9.9	11.1	Yoshikawa, Kochi, Japan
	16.0	11.3	0.41	0.91[b]	9.9	12.1	
	21.0	11.3	0.41	0.75[b]	9.2	10.2	
Williams (1973)	5.6	1.1*	0.78	0.15[b]	3.5	3.3	Stanley Bay, Hong Kong
	4.4	1.1*	0.78	0.15[b]	5	4.7	*Average value of 0.1–2 mm
	7.0	1.1*	0.78	0.10[b]	6	4.6	
	7.3	1.1*	0.78	0.15[b]	6	5.6	
	6.0	1.1*	0.78	0.15[b]	4	3.8	
	14.2	1.1*	0.78	0.20[b]	5	5.5	
	10.0	1.1*	0.78	0.10[b]	5.5	4.2	
	11.8	1.1*	0.78	0.10[b]	3.5	2.7	
	3.8	1.1*	0.78	0.25[b]	4	4.9	
	4.5	1.1*	0.78	0.15[b]	6	5.6	
	6.0	1.1*	0.78	0.15[b]	9	8.5	
	5.6	1.1*	0.78	0.15[b]	7.5	7.1	
	6.4	1.1*	0.78	0.10[b]	10	7.7	
	4.8	1.1*	0.78	0.25[b]	4	4.9	
Yamanouchi (1960)	16.8	0.32	0.88	0.33[b]	6	9.5	Takahagi, Ibaraki, Japan
	21.0	0.31	0.88	1.0[b]	11	30.2	Tokaimura, Ibaraki, Japan
	21.7	0.46	0.86	0.67[b]	8.6	19.0	
	20.3	0.5	0.85	0.56[b]	6	11.9	Kamogawa, Chiba, Japan
	27.3	0.52	0.85	0.78[b]	6	13.6	Chitose, Chiba, Japan
	6.3	0.27	0.89	0.15[b]	6	6.5	Tateyama, Chiba, Japan
	8	0.27	0.89	0.2[b]	4	5.0	
	4.8	0.27	0.89	0.2[b]	5	6.2	
	4.75	0.27	0.89	0.2[b]	6	7.5	Tomiura, Chiba, Japan
	7.7	0.78	0.81	0.2[b]	5.5	7.2	Fittsu, Chiba, Japan
	8	0.78	0.81	0.2[b]	5	6.5	
	9.3	0.78	0.81	0.3[b]	6	8.8	
	7.7	0.63	0.83	0.2[b]	4	4.7	Kashiwazaki, Niigata, Japan
	7.7	0.61	0.84	0.4[b]	4	6.6	
	20.7	0.55	0.84	0.5[b]	7.3	13.6	

[a] Shallow-water waves.
[b] Breaking waves.

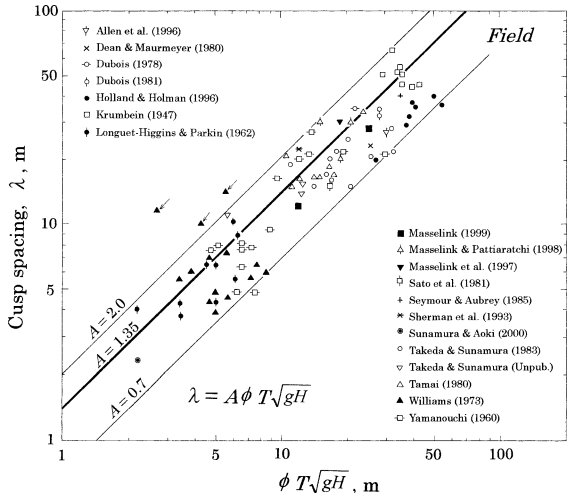

Fig. 5. Field relationship between the cusp spacing, λ, and the wave-sediment parameter, $\phi T\sqrt{gH}$.

p. 183). Calculation of wave height H at this location requires the determination of the height of incident waves in the area unaffected by diffraction, H_i, off the tip of Green Point (Location 'A' in Fig. 6c), where water depth is 5.9 m (=5.0+0.9 m). The wave height H_i was calculated through $H_i=K'_r K'_s H_o$, where K'_r and K'_s are the refraction and shoaling coefficients at Location A, respectively. Finally H was obtained from $H=K_d H_i$, with the result shown in Table 3.

The estimated wave height H is plotted against the alongshore distance x in Fig. 7a. It is found that waves in the exposed northern part are much higher than in the protected southern area. Visual observations of breaker heights by Masselink (1999) on the day of cusp measurements showed that they were approximately 1.25 and 0.25 m at the northern and southern sections of Pearl Beach, respectively. The present estimation and Masselink's observations are in fairly good agreement, although the field data are very limited in number.

Another parameter to be quantified for calculation of the cusp spacing using Eq. (9) is the sediment parameter ϕ that is a function of beach sediment size (Eq. (5)). Masselink (1999) also provided data on the size of sediment, sampled from the mid-beachface position at a certain interval of alongshore distance when cusp morphologies were measured. Fig. 7b shows the alongshore variation in sediment size, D, connecting Masselink's data by a line. Calculated values of ϕ using Eq. (5) are plotted in Fig. 7c. No marked spatial variation in ϕ-values is found.

Using data of H from Fig. 7a and ϕ from Fig. 7c, and substituting T=8.5 s into Eq. (9) with A=1.35, the cusp spacing λ was calculated. Fig. 7d plots these results along with the data from Masselink (1999). This figure demonstrates that the model can sufficiently describe a general trend of the alongshore variation in cusp spacings, although it does not explain minor fluctuations. Fig. 7a to d indicates that wave height is the most dominant controlling factor for cusp spacings along the shore. They also show that sediment grain size has only a slight influence on the cusp spacing of this beach in spite of the fact that the grain size changes significantly in the alongshore direction (from 0.2 to 0.8 mm). This is because the range of corresponding ϕ-values is small (from 0.90 to 0.82), suggesting that swash processes on such a beach composed of fine to coarse sands are not significantly affected by the grain size.

The dependence of cusp spacings on sediment size will be discussed using the previous field data. For this purpose, data of beach cusps that were formed under similar wave conditions (H=0.5–0.76 m and T=6–6.5 s) on beaches with quite different grain sizes were selected (Table 2): two from coarse-grained beaches, Chesil Beach, UK (Longuet-Higgins and Parkin, 1962) with D=14.0 mm and λ=8.8 m, and Manazuru, Japan (Sunamura and Aoki, 2000) with D=40 mm and λ=2.35 m; and two from fine-sand beaches, Portmore Beach, Ireland (Sherman et al., 1993) with D=0.2 mm and λ=22.5 m, and Naka Beach, Japan (Takeda and Sunamura, 1983) with D=0.28 mm and λ=15 m. The two kinds of data sets clearly indicate how strongly the grain size influences the spacing of beach cusps. Incidentally, calculation of cusp spacings using Eq. (9) with A=1.35 resulted in: λ=8.5 m for Chesil Beach, 3.0 m for Manazuru, 19.3 m for Portmore, and 19.2 m for Naka Beach. It is found that measurements and calculations are in fairly good agreement.

A large discrepancy is seen in the section around x=400 m between the calculated values and the field data (see Fig. 7d). This is due probably to the overestimation of wave height at this location. The wave refraction diagram is constructed on the assumption of conservation of wave energy between orthogonals, i.e., no lateral flows of energy along a wave crest. Actually in the field, however, lateral

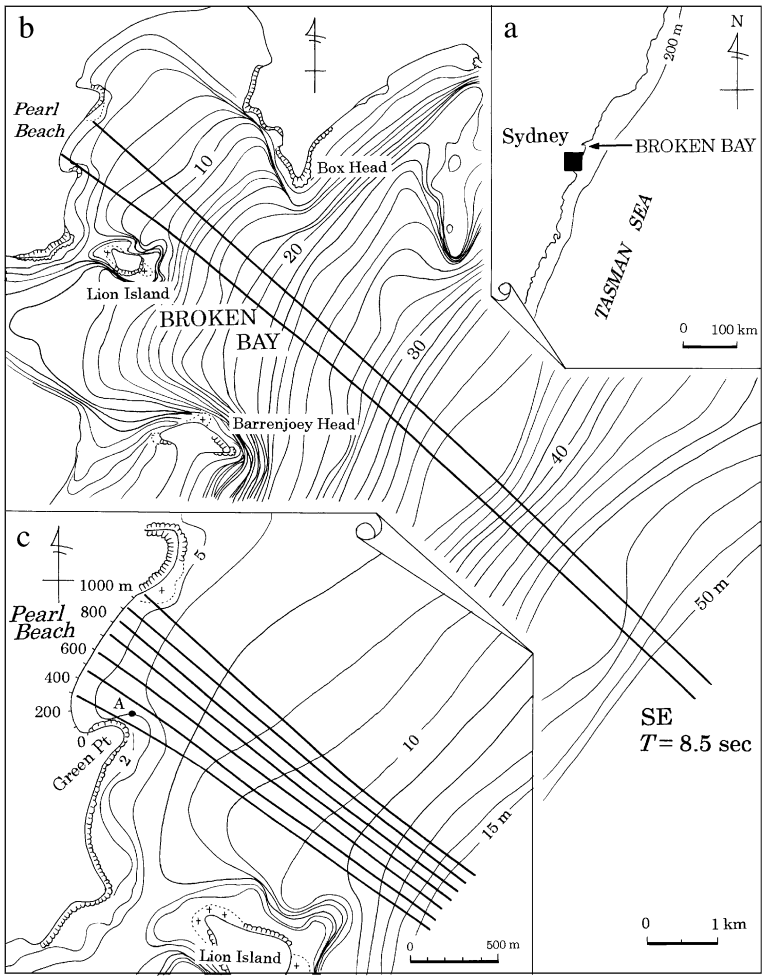

Fig. 6. Masselink's (1999) field site (Pearl Beach in Broken Bay, New South Wales, Australia) and wave refraction diagrams. (a) Location of Broken Bay; (b) refraction diagram for waves incident from SE with a period of 8.5 s; and (c) details in the region shallower than 15 m water depth.

energy-transmittance must have occurred through the southernmost orthogonal toward the sheltered zone located further south (see Fig. 6c), which resulted in significant decrease in wave height around x=400 m. Such wave height reduction was not considered here. Another discrepancy is found at the northernmost part of the beach. Fig. 7d shows that the measured cusp spacings decrease gradually from the location x=900 m to the extreme northern end which is adjacent to a rocky coast. In front of the rocky coast shore platforms develop jutting out into the sea, with rugged rock ledges located in very shallow water. Such topographical characteristics must have caused a considerable reduction in wave height around the northern end, resulting in the decrease in cusp spacings. The presence of the shore platforms was not taken into account in the wave height estimation of the present study.

6. Conclusions

Modeling based on water particle kinematics of horn-divergent uprush flow, incorporating a factor of

Table 3
Estimated results of nearshore wave height

x (m)	K_r	K_s	K_d	H (m)	Remarks
0	–	–	0.20	0.20	$H=K_dH_i$
100	–	–	0.23	0.22	(H_i=0.95 m[1])
200	–	–	0.37	0.35	
300	–	–	0.50	0.48	
400	0.55	1.26	–	1.0	$H=K_rK_sH_o$
550	0.62	1.26	–	1.2	(H_o=1.5 m)
670	0.65	1.26	–	1.2	
780	0.74	1.26	–	1.4	
880	0.77	1.26	–	1.5	
1000	0.65	1.26	–	1.2	

$H_i=K'_rK'_sH_o$=0.62×1.02×1.5 m=0.95 m.

sediment grain size, yielded Eq. (9). The value of A in this equation was determined by using numerous sources of field data (Fig. 5). Eq. (9) with A=1.35 enables prediction of the spacing of beach cusps in the field from wave height, period, and sediment parameter (ϕ in Eq. (5)). Applicability of this predictive relation was examined using Masselink's (1999) field data. The result indicated that the relation is capable of more than adequately explaining a general trend of the alongshore variation in cusp spacings at Pearl Beach in New South Wales (Fig. 7d).

List of symbols

A	coefficient (=2aB)
a	coefficient (=λ/l_*)
B	coefficient (=2$k$sin2θ)
D	sediment grain size
f	coefficient (=λ/S)
g	gravitational acceleration
H	nearshore wave height
H_b	breaking wave height
H_i	incident wave height
H_o	deepwater wave height
K_d	diffraction coefficient
K_r, K'_r	refraction coefficient
K_s, K'_s	shoaling coefficient
k	coefficient
l	maximum alongshore displacement of water particle obliquely rushing up on an impermeable, smooth beach
l_*	maximum alongshore displacement of water particle obliquely rushing up on a permeable, rough beach
m	type of zero-mode edge waves (m=1: subharmonic, m=2: synchronous)
R	maximum runup height of waves normal to a beach

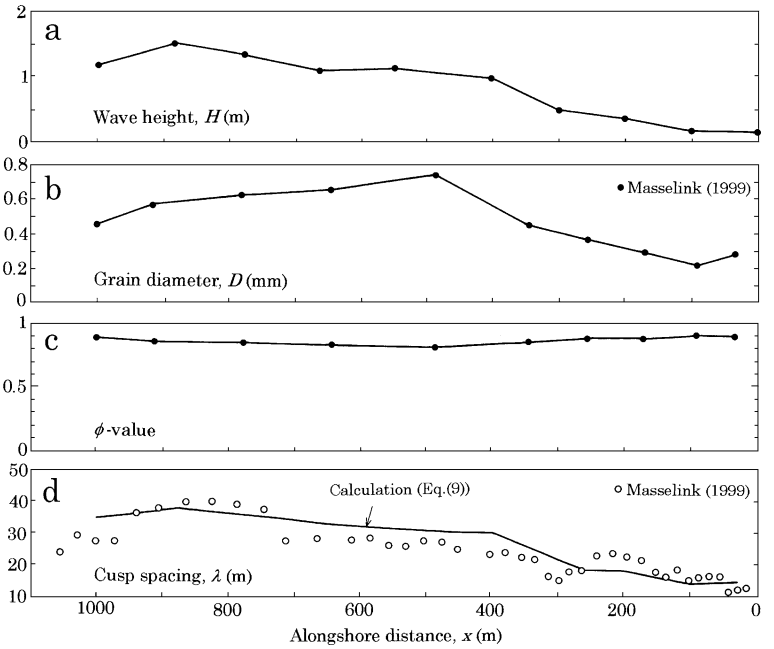

Fig. 7. Alongshore variations of: (a) estimated wave height, (b) sediment grain size, (c) ϕ-value, and (d) calculated cusp spacing.

S swash excursion length
T wave period
V initial velocity of water particle
β beach slope angle
η maximum cusp indentation
θ initial angle of deflected trajectory of water particle rushing up on a uniformly sloping beach
λ spacing of beach cusps
ρ density of water
ϕ coefficient representing the effectiveness of beach sediment in dissipating runup wave energy

Acknowledgements

Fruitful comments given by anonymous reviewers enhanced this paper. Financial support from Lab Costa (President: Sadakazu Katori) is greatly appreciated. Hidekazu Tsujimoto of Osaka Kyoiku University provided useful information on Pearl Beach and its vicinity, and Junko Murata, nee Karashima, assisted me in preparing the manuscript.

References

Aagaard, T., 1985. Observations of beach cusps. Geografisk Tidsskrift 85, 27–31.

Allen, J.P., Psuty, N.P., Bauer, B.O., Carter, R.W.G., 1996. A field data assessment of contemporary models of beach cusp formation. Journal of Coastal Research 12, 622–629.

Aoki, H., Sunamura, T., 2000. A laboratory experiment on the formation and morphology of beach cusps. Transactions, Japanese Geomorphological Union 21, 291–306.

Australian Hydrographic Office, 1977. Hydrographic chart "Broken Bay" (Scale 1:40 000), Hydrographic Service, Royal Australian Navy, Wollongong, N.S.W.

Bagnold, R.A., 1940. Beach formation by waves: some model experiment in a wave tank. Journal of Institute of Civil Engineers 15, 27–52.

Coastal Engineering Research Center, 1984. Shore Protection Manual vol. 1. U.S. Army Corps of Engineers, Washington, DC.

Coco, G., O'Hara, T.J., Huntley, D.A., 1999. Beach cusps: a comparison of data and theories for their formation. Journal of Coastal Research 15, 741–749.

Coco, G., Huntley, D.A., O'Hara, T.J., 1999. Regularity and randomness in the formation of beach cusps. Marine Geology 178, 1–9.

Coco, G., Huntley, D.A., O'Hara, T.J., 2000. Investigation of a self-organization model for beach cusp formation and development. Journal of Geophysical Research 105, 21991–22002.

Coco, G., Burnet, T.K., Werner, B.T., 2003. Test of self-organization in beach cusp formation. Journal of Geophysical Research 108 (3101), 46-1–46-11.

Dalrymple, R.L., Lanan, G.A., 1976. Beach cusps formed by intersecting waves. Geological Society of America Bulletin 87, 57–60.

Dean, R.G., Maurmeyer, E.M., 1980. Beach cusps at Point Reyes and Drakes Bay beaches, California. Proceedings of 17th International Conference on Coastal Engineering. American Society of Civil Engineers, pp. 863–884.

Dubois, R.N., 1978. Beach topography and beach cusps. Geological Society of America Bulletin 89, 1133–1139.

Guza, R.T., Inman, D.L., 1975. Edge waves and beach cusps. Journal of Geophysical Research 80, 2997–3012.

Guza, R.T., Bowen, A.J., 1981. On the amplitude of beach cusps. Journal of Geophysical Research 86, 4125–4132.

Holland, K.T., Holman, R.A., 1996. Field observations of beach cusps and swash motions. Marine Geology 134, 77–93.

Hunt Jr., I.A., 1959. Design of seawalls and breakwaters. Journal of Waterways Harbors Division, American Society of Civil Engineers 85, 123–152.

Huntley, D.A., Bowen, A.J., 1978. Beach cusps and edge waves. Proceedings of 16th International Conference on Coastal Engineering, American Society of Civil Engineers, 1378–1393.

Inman, D.L., Guza, R.T., 1982. The origin of swash cusps on beaches. Marine Geology 49, 133–148.

Johnson, D.W., 1910. Beach cusps. Geological Society of America Bulletin 21, 599–624.

Kaneko, A., 1985. Formation of beach cusps in a wave tank. Coastal Engineering 9, 81–98.

Kuenen, P.H., 1948. The formation of beach cusps. Journal of Geology 56, 34–40.

Longuet-Higgins, M.S., Parkin, D.W., 1962. Sea waves and beach cusps. Geographical Journal 128, 194–201.

Masselink, G., 1999. Alongshore variation in beach cusp morphology in a coastal embayment. Earth Surface Processes and Landforms 24, 335–347.

Masselink, G., Pattiaratchi, C.B., 1998. Morphological evolution of beach cusps and associated swash circulation patterns. Marine Geology 146, 93–113.

Masselink, G., Hegge, B.J., Pattiaratchi, C.B., 1997. Beach cusp morphodynamics. Earth Surface Processes and Landforms 22, 1139–1155.

Miller, J.R., Miller, S.M.O., Torzynski, C.A., Kochel, R.C., 1989. Beach cusp destruction, formation, and evolution during and subsequent to an extratropical storm, Duck, North Carolina. Journal of Geology 97, 749–760.

Nolan, T.J., Kirk, R.M., Shulmeister, J., 1999. Beach cusp morphology on sand and mixed sand and gravel beaches, South Island, New Zealand. Marine Geology 157, 185–198.

Palmer, H.R., 1834. Observations on the motions of shingle beaches. Philosophical Transactions Royal Society of London 124, 567–576.

Pyökäri, M., 1982. Breaching of a beach ridge and the formation of beach cusps. Canadian Geographer 26, 332–348.

Russell, R.J., McIntire, W.G., 1965. Beach cusps. Geological Society of America Bulletin 76, 307–320.

Sallenger, A.H., 1979. Beach cusp formation. Marine Geology 29, 23–37.

Savage, R.P., 1959. Laboratory Data on Wave Run-Up on Roughened and Permeable Slopes. U.S. Army Corps of Engineers, Beach Erosion Board, Washington, DC. Technical Memorandum, No. 109, 28 pp.

Seymour, R.J., Aubrey, D.G., 1985. Rhythmic beach cusp formation: a conceptual synthesis. Marine Geology 65, 289–303.

Sherman, D.J., Orford, J.D., Carter, R.W.G., 1993. Development of cusp-related, gravel size and shape facies at Malin Head, Ireland. Sedimentology 40, 1139–1152.

Sunamura, T., 1984. Quantitative predictions of beach-face slopes. Geological Society of America Bulletin 95, 242–245.

Sunamura, T., 1989. Sandy beach geomorphology elucidated by laboratory modeling. In: Lakhan, V.C., Trenhaile, A.S. (Eds.), Applications in Coastal Modeling. Elsevier, Amsterdam, pp. 159–213.

Sunamura, T., Aoki, H., 2000. A field experiment of cusp formation on a coarse clastic beach using a suspended video-camera system. Earth Surface Processes and Landforms 25, 329–333.

Takeda, I., Sunamura, T., 1983. Formation and spacing of beach cusps. Coastal Engineering in Japan 26, 121–135.

Takeda, I., Terasaki, T., Sunamura, T., 1986. Formation and spacing of beach cusps on a laboratory beach. Annual Report of Institute of Geoscience vol. 12, pp. 55–58. University of Tsukuba.

Werner, B.T., Fink, T.M., 1993. Beach cusps as self-organized patterns. Science 260, 968–971.

Wiegel, R.L., 1964. Oceanographic Engineering. Prentice-Hall, Englewood Cliffs, NJ. 532 pp.

Williams, A.T., 1973. The problem of beach cusp development. Journal of Sedimentary Petrology 43, 857–866.